Seismic Performance and Modeling of Post-Tensioned, Precast Concrete Shear Walls

A.C. Tanyeri & J.P. Moehle
University of California, Berkeley, USA

T. Nagae
National Research Institute for Earth Science and Disaster Prevention, Miki City, Japan

15 WCEE
LISBOA 2012

SUMMARY:
A three-dimensional earthquake simulation test on a full-scale, four-story, prestressed concrete building was conducted using the E-Defense shaking table facility. The seismic force-resisting system of the test building comprised two post-tensioned (PT) frames in one direction and two unbonded PT precast walls in the other direction. The test building was subjected to several earthquake ground motions, ranging from serviceability level to near collapse. The behavior of the wall direction of the building under several ground motions is simulated using nonlinear response history analysis of practical structural engineering models, and the 2D simulation results are compared with the test results. Conducted analytical simulations are in good correlation with the test results for the important engineering parameters with some discrepancies.

Keywords: Earthquake simulation test, Seismic, Shearwall, Structural wall, Precast concrete

1. INTRODUCTION

Past earthquakes have shown examples of unsatisfactory performance of buildings using reinforced concrete structural walls as the primary lateral force-resisting system. In the 1994 Northridge earthquake examples can be found where walls possessed too much overstrength, leading to unintended failure of collectors and floor systems, including precast and post-tensioned construction. In the 2010 Chile and 2011 Christchurch earthquakes, many structural wall buildings sustained severe damage. Although some differences in detailing practices exist between those countries and the U.S., the failure patterns raise concerns about how well conventionally reinforced structural walls in U.S. buildings will perform during the next earthquake. Past research efforts, including the PREcast Seismic Structural Systems (PRESSS) program (Priestley 1991) and subsequent studies, have explored alternative design approaches using post-tensioned (PT) precast structural walls to better control yielding mechanisms and promote self-centering behavior. These studies have provided excellent guidance on design and construction requirements, but examples of full-scale, three-dimensional dynamic tests to demonstrate behavior in realistic structural systems have been lacking. Such demonstrations are important to identify complex interactions that occur in complete building structures. Such demonstrations also are useful to serve as a vehicle for acceptance by the engineering community.

In December 2010, the National Research Institute for Earth Science and Disaster Prevention (NIED) in Japan conducted a three-dimensional earthquake simulation test on a full-scale, four-story building using the E-Defense shaking table. Design, instrumentation, preliminary analytical studies, and testing of the building were a collaboration among researchers from Japan and the U.S. The seismic force-resisting system of the test building comprised two bonded PT frames in one direction and two unbonded PT precast walls in the other direction. The building was designed using the latest code requirements and design recommendations available both in Japan and the U.S., including the ACI ITG-5.2-09. The test building was subjected to several earthquake ground motions, ranging from serviceability level to near collapse.

Three-dimensional earthquake simulation testing of full-scale specimens is rare. Data from this test give a unique opportunity to understand the behavior of the unbonded PT walls and their interaction with other structural elements during an earthquake. In this study, the authors developed practical structural engineering models for the wall direction of the building. A comparison of the simulation and test results is done to assess the capability of currently available models to simulate the response of a real PT building under gradually increasing earthquakes.

2. OVERVIEW OF THE TEST

2.1. Test Specimen

The test specimen was a full-scale, four-story, post-tensioned precast concrete building. It had a rectangular plan (Fig 1), with dimensions 7.2 m in Y (transverse) direction and 14.4 m in X (longitudinal) direction. Height of each floor was 3 m, resulting in total building height of 12 m. The lateral-load-resisting system in Y direction was two precast unbonded PT shear walls and one bay unbonded PT center frame at B Axis. In X direction the structural system consisted of two bay bonded PT frames. All the structural elements were precasted off-site and installed and post-tensioned on-site. Post-tensioning tendons of beams and columns in X direction were bonded with grouting after installation. On the other hand, PT tendons of shearwalls and beams in Y direction were constructed to be unbonded from concrete.
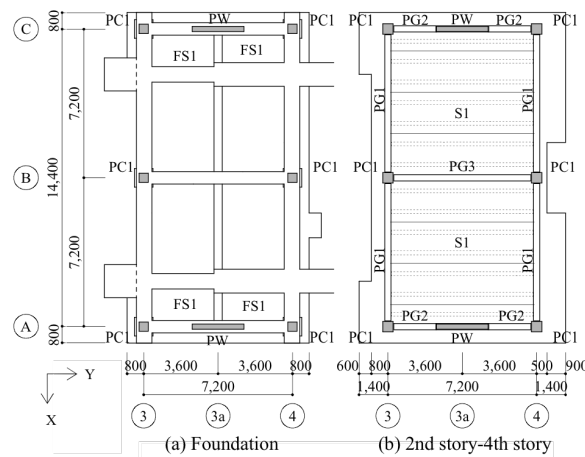

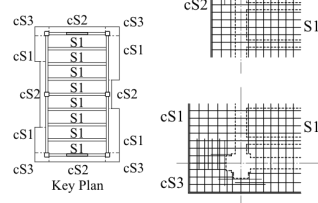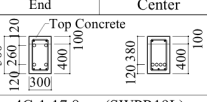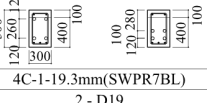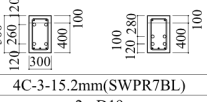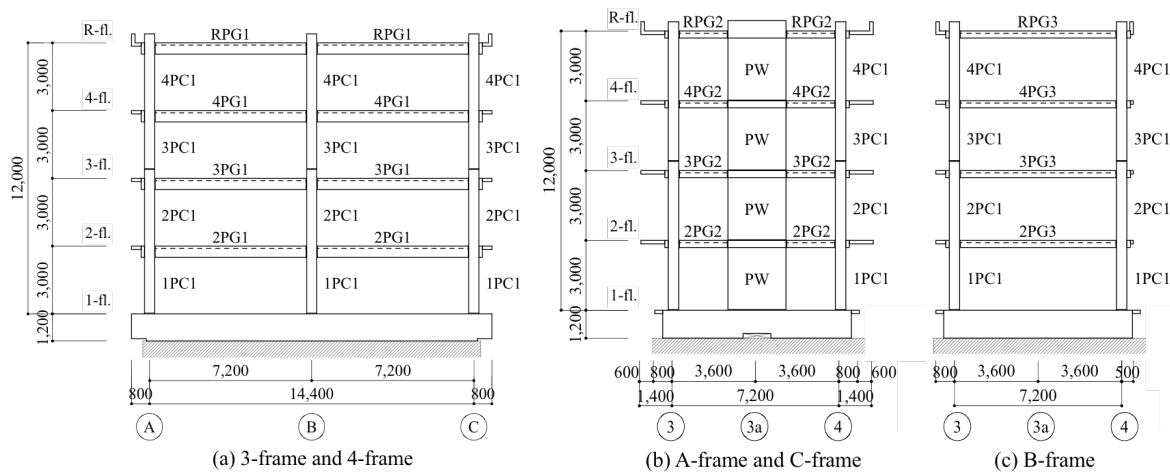**Figure 1.** Floor plan of the specimen (Unit: mm)

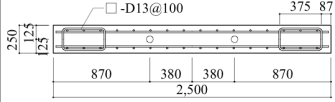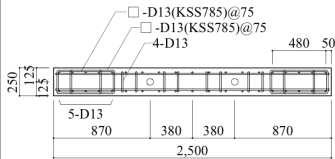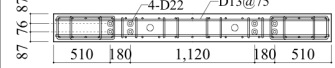**Figure 2.** Elevation view of the specimen (Unit: mm)

Shearwalls had a rectangular cross-section with a length of 2500 mm and a thickness of 250 mm. PT walls were 12 m high, and therefore had a slenderness ratio of $H_w/l_w = 4.8$. Columns (PC1) were square and dimensioned 450 mm by 450 mm. Beams (PG2 & PG3) were partially precast, with the top 100 mm of the 300mm by 300 mm section cast-in-place with the slab. The slab was 130 mm thick with top 100 mm cast on site monolithically with the beams. The slab was supported by pretensioned joists with 1 m interval in the transverse direction. See Table 1 for additional details (Nagae et al. 2011).

Table 1 Member Cross-sections

List of Column

		PC1
All	Section	
	Tendon	8-21mm(SBPR1080/1230)
	Rebar	4-D19
	Hoop	D10@100

List of Slab — Depth: 130mm

		Shorter direction	Longer direction
S1		D10@200	D10@200
cS1	Top	D13@200	D10@250
	Bottom	D10@200	D10@250
cS2	Top	D10@200	D10@250
	Bottom	D10@200	D10@250
cS3	Top	D13@200	D13@200
	Bottom	D10@200	D10@200

List of Girder

			PG1	
	Location		End	Center
R-fl.	Section			
	Tendon		4C-1-17.8mm(SWPR19L)	
	Top		2 - D19	
	Bottom		3 - D19	
	Stirrup		2-D10@150	2-D10@200
4-fl.	Section			
	Tendon		4C-1-19.3mm(SWPR7BL)	
	Top		2 - D19	
	Bottom		3 - D19	
	Stirrup		2-D10@100	2-D10@200
3-fl. 2-fl.	Section			
	Tendon		4C-3-15.2mm(SWPR7BL)	
	Top		2 - D19	
	Bottom		3 - D19	
	Stirrup		2-D10@90	2-D10@200

List of Girder

		PG2	PG3
All	Section		
	Tendon	2C-1-17.8mm(SWPR19L)	2C-1-17.8mm(SWPR19L) 1C-17mm(SBPR930/1080)
	Top	2 - D19	2 - D19
	Bottom	2 - D19	2 - D19
	Stirrup	2-D10@100(KSS785)	2-D10@150

List of Wall

		PW
4-fl. 3-fl. 2-fl.	Section	
	Tendon	3-10-15.2mm(SWPR7B)
	V bar	D13@150(double)
	H bar	D13@100(double)
1-fl.	Top Section	
	Bottom Section	
	Tendon	2-10-15.2mm(SWPR7B)
	V bar	D13@150(double)
	H bar	D13@75(double)

(Unit: mm)

Table 2 Effective prestress and permanent axial load

	P_e [kN]	N_L [kN]
1PC1 (B-axis)	2274	733
1PW	2666	176
2PG1	1822	-
2PG2	338	-
2PG3	338	-

Concrete design strength was 60 MPa for precast parts and 30 MPa for cast-in-place parts. The design strength of the grout mortar was 60 MPa. First two floors of north wall were constructed using FRCC (fiber reinforced cement composite). Nominal strength of the generic steel bar was 345 MPa. Transverse reinforcement of beams and walls in Y direction was high strength steel bars with nominal strength of 785 MPa. Although columns were designed for required shear reinforcement by the Japanese Building Standard Law, column core was not confined. PT rods of columns were high strength steel with 1080 MPa design strength. PT strands used in walls and beams had design strength of 1600 MPa. Test results of the materials are shown in Table 2.

Table 2 Material test results

<table>
<tr><th colspan="2">(a) Concrete</th><th></th><th colspan="2">(b) Grout</th></tr>
<tr><td></td><td>σ_B [N/mm^2]</td><td></td><td></td><td>σ_B [N/mm^2]</td></tr>
<tr><td>PCa</td><td>83.2</td><td></td><td>Mortar</td><td>135.6</td></tr>
<tr><td>PCa (F)</td><td>85.5</td><td></td><td>Mortar (F)</td><td>120.3</td></tr>
<tr><td>Top</td><td>40.9</td><td></td><td>Milk cement</td><td>63.4</td></tr>
</table>

(c) Steel

	σ_y [N/mm^2]	σ_t [N/mm^2]
PC bar φ21 (Column, SBPR1080/1230)	1194	1277
D22 (Wall, SD345)	385	563
D19 (Column and beam, SD345)	389	561
D13 (Wall, SD295A)	347	501
D13 (Slab, SD295A)	372	522
D10 (Column and beam, SD295A)	361	518
D10 (Slab, SD295A)	388	513
D13 (Wall and PG2, KSS785)	938	1107
	F_y [kN]	F_t [kN]
PC wire φ15.2 (Wall, SWPR7BL)	250	277
PC wire φ15.2 (Beam, SWPR7BL)	255	279
PC wire φ17.8 (Beam, SWPR19L)	356	404
PC wire φ19.3 (Beam, SWPR7BL)	429	481

Reinforcement details of PT walls and wall-to-beam joint details are shown in Figure 3. Total of 8 D22 (22 mm diameter) energy dissipation bars were unbonded through the lower 1.5 m of the first story and connected to the foundation with mechanical couplers. Effective prestressing of PT tendon was 0.6 times the yield strength for walls and PG2 beams, and 0.8 times the yield strength for the other beams and columns.
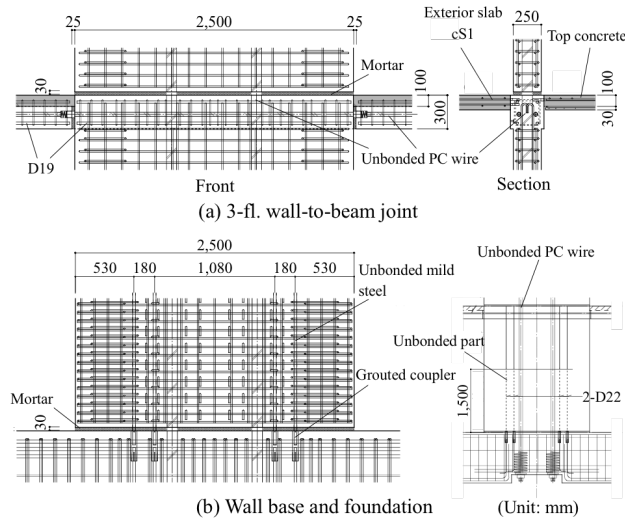
Figure 3. Reinforcement Details of Walls (Unit: mm)

The total weight of the specimen was 5592 kN. The weight of each floor was 996 kN for Roof, 813 kN for 3rd floor, 806 kN for 2nd floor and 804 kN for the 1st floor.

2.2. Input Motions

Input ground motions were scaled JMA-Kobe and JR-Takatori records from 1995 Kobe earthquake. Excitation was applied in two horizontal and vertical directions simultaneously. Firstly, JMA-Kobe motion was applied with wave amplitude magnification of 10%, 25%, 50%, and 100%, respectively. Lastly, 40% and 60% JR-Takatori were applied. In this paper we consider the 25%, 50% and 100% excitations only. Figure 4 shows time series and acceleration response spectra of input motions.
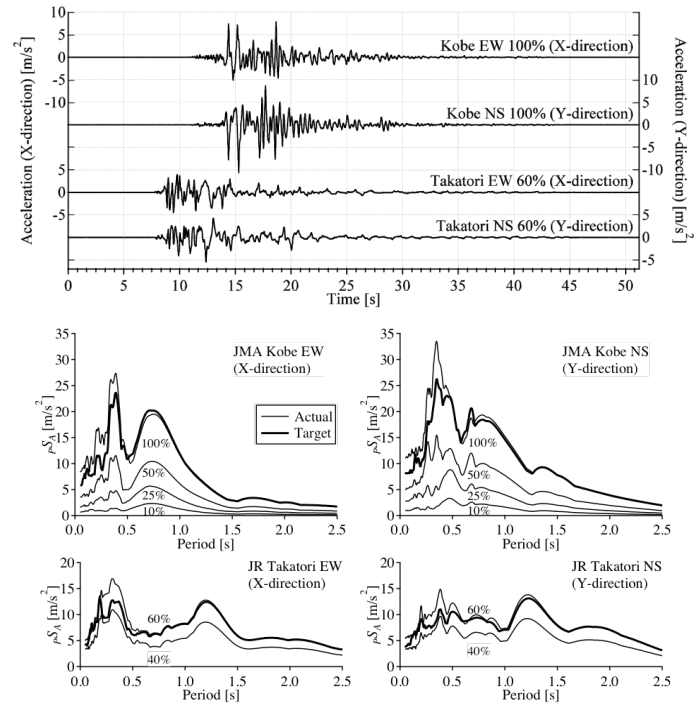
Figure 4. Time series and acceleration response spectra of input motions

3. ANALYTICAL SIMULATION

A three-dimensional analytical model of the Y direction of the specimen was implemented using computer program Perform 3D (CSI). Figure 5 shows a 3D view of the model.
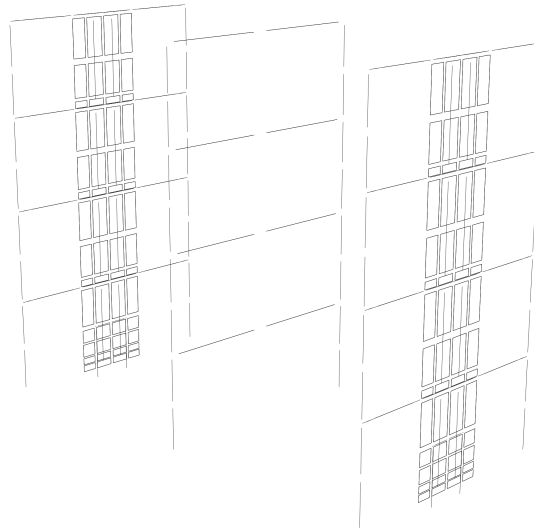

Figure 5. 3D view of the Perform 3D model

3.1. Shear Wall Model

Structural walls were modeled using 4-noded "Shear Wall Elements" (CSI) with fiber cross sections. In this implementation, all interconnected planar wall segments at any level are assumed to remain plane when deformed. In the first story, where inelastic actions were expected to concentrate, shear wall elements were meshed so that each element had a height of $2b_w$ (b_w = wall thickness). This value

is established from post-earthquake observations of the typical height of spalled regions. For the rest of the building, larger sized elements are used. Due to anticipated low shear demands, an elastic shear material was used for walls, with effective shear stiffness defined as $G_cA_w = 0.4E_cA_w/20$ (PEER/ATC-72-1), in which G_c is shear modulus, E_c is Young's modulus of concrete (taken as $4700\sqrt{f_c'}$, MPa), and A_w is web area. Rocking behavior of wall segments is implemented for wall elements at each floor level. This behavior is achieved through modifying material models assigned to fiber sections to have no tension resistance, keeping the compression stress-strain relationship same.

Constitutive material model for concrete is an idealization of material tests using a trilinear curve with a descending portion (Figure 6). Stress-strain relationship for confined concrete is implemented using the confinement model for high-strength concrete developed by Razvi & Saatcioglu (1999). Tension resistance of concrete is modeled except for the rocking sections.
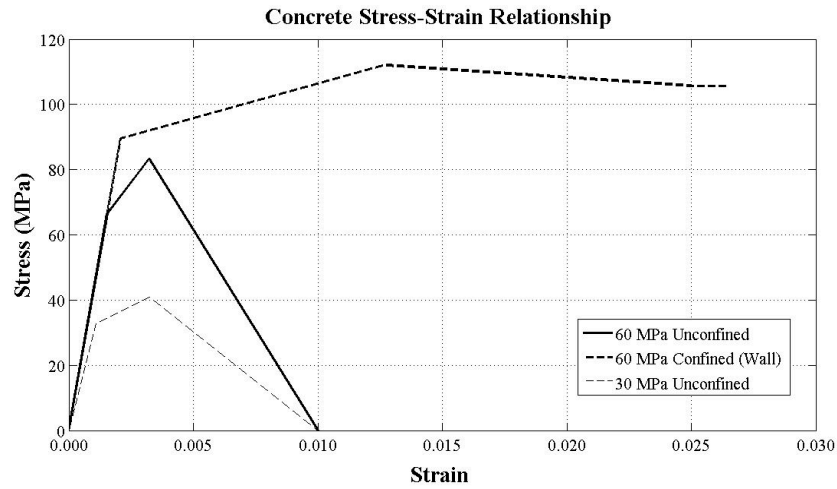

Figure 6. Concrete stress-strain relation

Similarly, the reinforcing steel stress-strain relation was a simplified trilinear curve with a descending portion (Figure 7). The ultimate strain of reinforcing steel in tension was limited to 0.05 in consideration of cyclic fatigue (PEER/ATC-72-1). Behavior in compression was checked according to the ratio s/d_b (s = spacing of transverse reinforcement and d_b = diameter of longitudinal bar) in consideration of longitudinal bar buckling (Monti and Nuti, 1992). The adequately small s/d_b ratio is such that reinforcing bars are unlikely to buckle prematurely. The ultimate strain of reinforcing steel under compression is limited to 0.02 (PEER/ATC-72-1).
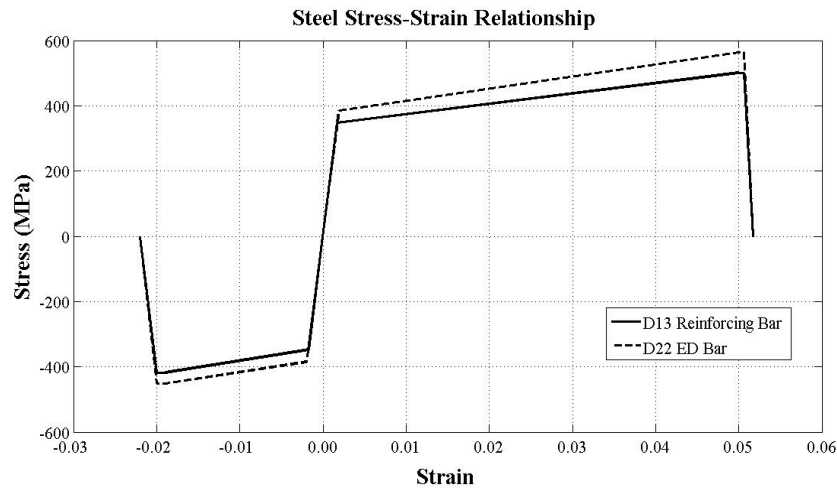

Figure 7. Reinforcing stress-strain relation

PT tendons and energy dissipation (ED) bars are modelled using truss elements with nonlinear material properties. Truss elements are connected to shear wall elements through rigid beams extending to locations of tendons and ED bars in section. Lateral displacements of PT tendons are slaved to shear wall elements at each floor level, which is analogous to the effect of tendon ducts. Truss elements representing ED bars are modelled along the unbonded length of the bars. Bar slip (strain penetration) effects are considered for modelling of ED bars. ED bar trusses are extended below top of foundation to mimic the extra elongation caused by the slip of ED bars. Post-tensioning loads on tendons are applied as initial strains consequently with gravity loads in analysis.

3.2. Beam and Column Models

Beams and columns are modelled using nonlinear beam column elements with rigid end zones. Nonlinear fiber sections are assigned through the length of elements with distributed plasticity. Similar to the shear wall elements, a simplified trilinear curve with a descending portion is used to model concrete and steel materials. Due to adequate shear design of the members, an elastic shear material was used for beams and columns, with effective shear stiffness defined as $G_cA_w = 0.4E_cA_w$ (Elwood et al. 2007). Similar to rocking sections of wall elements, opening between precast elements is simulated by assigning a "rocking section" to necessary integration points of elements (i.e., closest integration point of a beam element to a wall or column). Aforementioned "rocking section" has the same cross-section and fiber locations with other integration points. However, materials assigned to this section are modified to have no tension resistance, keeping the compression response unchanged.

Upper portions of half-precast beams were cast monolithic with slabs. Beam effective flange widths are calculated using ACI 318 equations. Unlike column elements, for which forces are resisted with fiber sections in both transverse directions, beam elements in Perform 3D use fiber sections only in the major bending axis. Bending stiffness of the minor bending axis is defined with effective bending stiffness as $0.5E_cI_g$, in which I_g is gross section moment of inertia according to the minor bending axis.

Unbonded PT tendons of beams (PG2 & PG3) are modelled with parallel truss elements with nonlinear material properties. Their vertical displacements through beams and walls are slaved to parallel elements similar to modelling of ducts for walls. Similar to PT tendons of walls, post-tensioning loads on tendons are applied as initial strains. In contrast, bonded PT rods of columns (PC1) are included in the fiber cross-section. Post-tensioning loads on columns are approximated by applied point loads (in the same direction with gravity).

3.3. Miscellaneous Notes on the Analytical Model

Rayleigh damping is used for nonlinear response history analysis, with parameters set to produce 2 percent damping at periods $0.2T_1$ and T_1, where $T_1 = 0.29$ seconds. All analyses were in Y direction, therefore X direction displacements of all nodes are restrained. After the application of gravity and prestressing loads, the model is excited with 25%, 50%, and 100% Kobe motions, respectively.

4. COMPARISON OF SIMULATION AND TEST RESULTS

Prior to application of earthquake motions, the test building was excited with white noise. Fundamental periods of the building were 0.29 s in Y direction and 0.45 s in X direction. Modal analysis of the analytical model resulted a fundamental period of 0.29 s in Y direction.

Base shear versus roof drift ratio responses of the analytical model and test specimen under 25%, 50%, 100% Kobe excitations are shown in Figures 8, 10, and 12. Comparisons of roof drift ratio versus time responses of analytical model and test specimen are shown in Figures 9, 11, and 13. Flag-shaped hysteresis typical of unbonded post-tensioned concrete is apparent. Analytical model and test results are in very good agreement for important engineering parameters, such as stiffness, maximum base shear, and maximum roof drift. For all excitations, energy dissipated during the earthquake (area

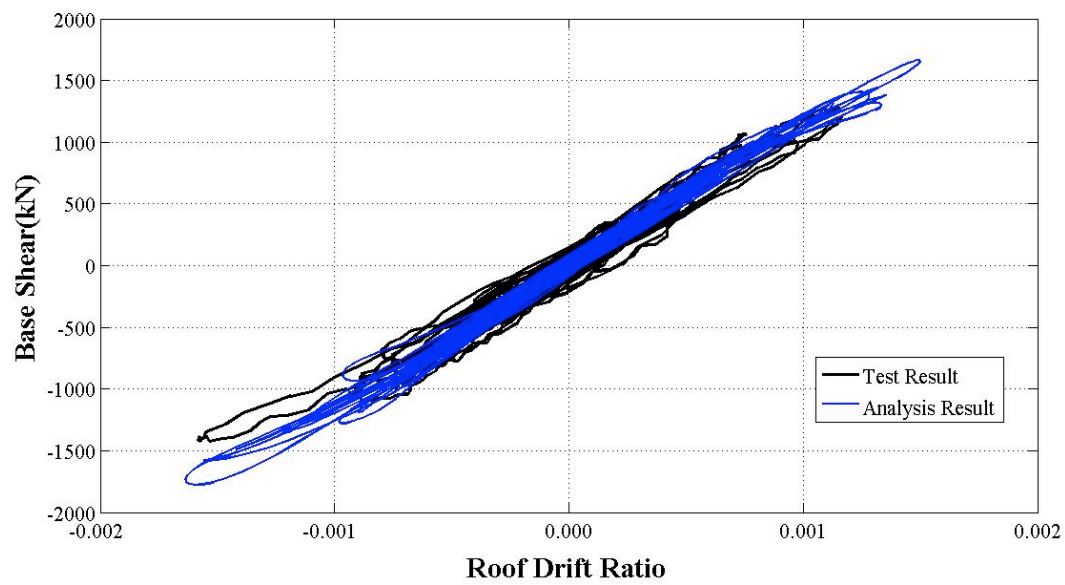inside the hysteresis curve) is estimated with a good accuracy.

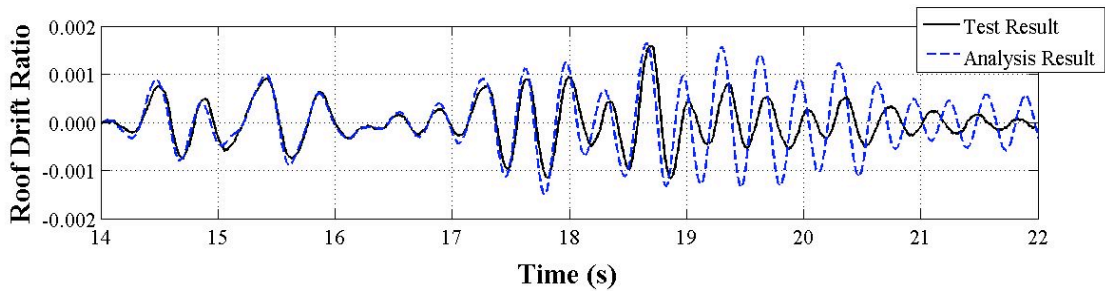**Figure 8.** Base Shear-Roof Drift Ratio comparison of results for 25% Kobe motion

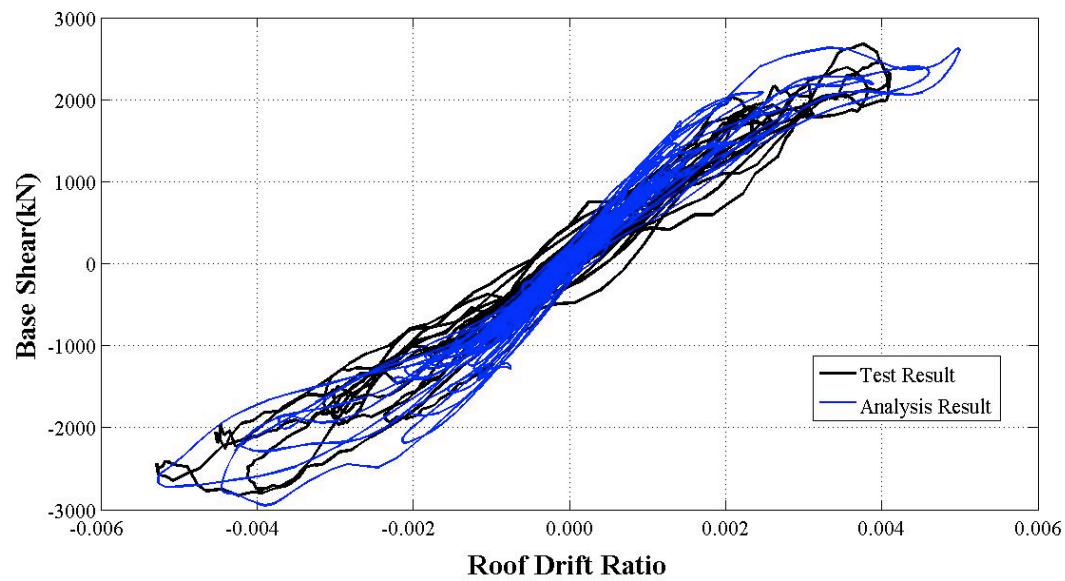**Figure 9.** Roof Drift Ratio-Time comparison of results for 25% Kobe motion

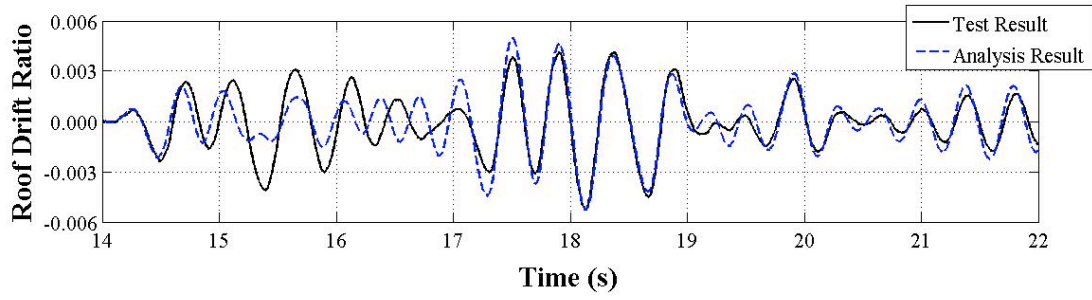**Figure 10.** Base Shear-Roof Drift Ratio comparison of results for 50% Kobe motion

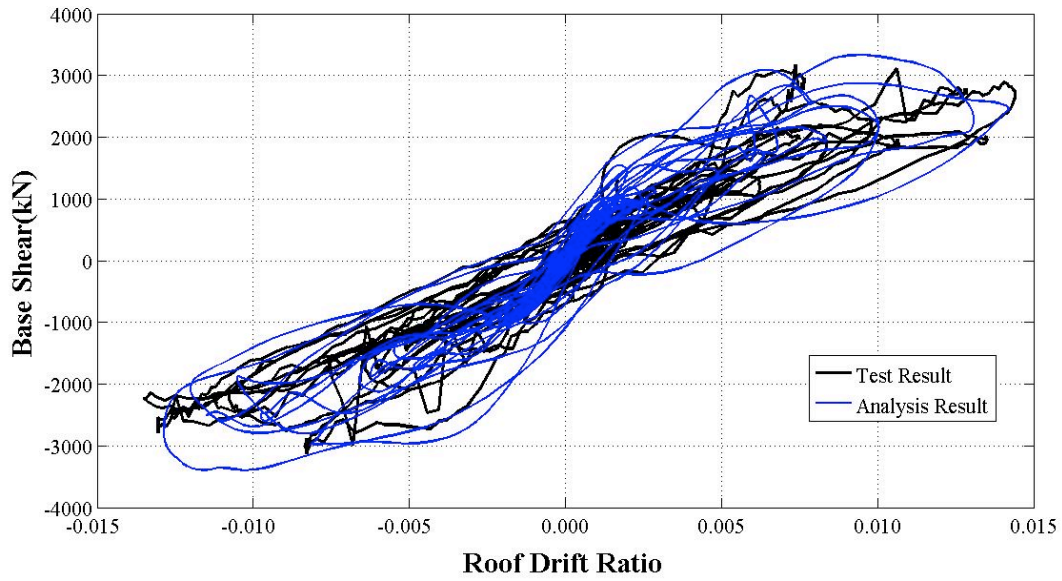**Figure 11.** Roof Drift Ratio-Time comparison of results for 50% Kobe motion

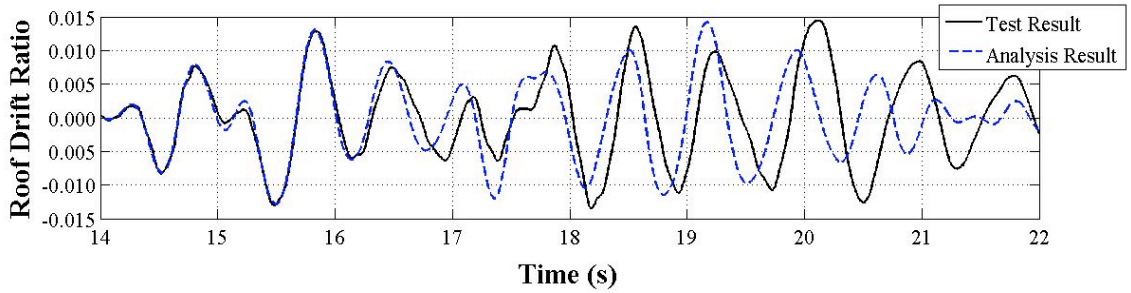**Figure 12.** Base Shear-Roof Drift Ratio comparison of results for 100% Kobe motion

Figure 13. Roof Drift Ratio-Time comparison of results for 100% Kobe motion

Although estimated maximum roof drift ratios are very close to the test results, phase shifts in roof drift ratio versus time series are significant for some parts of response. Roof drift ratio time history estimate for 25% Kobe motion is shifting out-of-phase after 19 s. Vibration period of test specimen is increasing after 19 s, but the analytical model does not identify this increase in period. Calculated roof drift ratio history for 100% motion also does not estimate the increase in vibration period after 16 s.

Assumed damping for the analytical model is having a good agreement for the response of 50% Kobe excitation. For 25% motion response, calculated response damps out more slowly than the test results. Estimated roof drift ratio response damps out faster than the test results for 100% motion.

5. CONCLUSIONS

A three-dimensional earthquake simulation test on a full-scale, four-story, prestressed concrete building is conducted using the E-Defense shaking table facility. The seismic force-resisting system of the test building comprised two post-tensioned (PT) frames in one direction and two unbonded PT precast walls in the other direction. The test building was subjected to several earthquake ground motions, ranging from serviceability level to near collapse. The wall direction (Y direction) of the building is modeled using the computer program Perform 3D, with emphasis on an implementation that would be practical for design-office implementation. This model is subjected to several ground motions to explore the accuracy of the analytical model.

Important engineering parameters such as fundamental vibration period, stiffness, hysteresis shape, maximum base shear, and maximum roof drifts are adequately simulated using the analytical model. There are, however, some discrepancies in variation of these responses with time. These results indicate that, while further improvements may be desirable, the selected modelling approach is capable of producing seismic response estimates of sufficient accuracy to be used for detailed design of unbonded post-tensioned, precast structural wall systems.

REFERENCES

ACI 318-08 (2008). Building Code Requirements for Structural Concerete (ACI 318-08) and Commentary, American Concrete Institute, Farmington Hills, Michigan

ACI ITG-5.2-09 (2009). Requirements for Design of a Special Unbonded Post-Tensioned Precast Shear Wall Satisfying ACI ITG-5.1 (ACI ITG-5.2-09) and Commentary, American Concrete Institute, Farmington Hills, Michigan

Computers and Structures, Incorporated (CSI), Perform 3D, Nonlinear Analysis and Performance Assesment for 3D Structures.

Elwood, K.J., Matamoros, A.B., Wallace, J.W., Lehman, D.E., Heintz, J.A., Mitchell, A.D., Moore, M.A., Valley, M.T., Lowes, L.N., Comartin, C.D., and Moehle, J.P. (2007). Update to ASCE/SEI 41 Concrete Provisions. *Earthquake Spectra.* **23:3**,493-523.

Nagae, T., Tahara, K., Matsumori T., Shiohara, H., Kabeyasawa T., Kono, S., Nishiyama, M., Wallace, J., Ghannoum, W., Moehle, J.P., Sause R., Keller, W., and Tuna, Z. (2011). Design and Instrumentation of the 2010 E-Defense Four-Story Reinforced Concrete and Post-Tensioned Concrete Buildings. *Technical Report 2011/104, Pacific Earthquake Engineering Research Center,* University of California, Berkeley

Monti, G., and Nuti, C. (1992). Nonlinear Cyclic Behavior of Reinforcing Bars Including Buckling. *Journal of Structural Engineering,* ASCE, **118:12**,3268-3284.

PEER/ATC-72-1 (2010). Modeling and Acceptance Criteria for Seismic Design and Analysis of Tall Buildings, Applied Technology Council, Redwood City, CA.

Priestley, M.J.N. (1991). Overview of the PRESSS research program. *PCI Journal.* **41:2**,22-40.

Razvi, S., and Saatcioglu, M. (1999). Confinement Model for High-Strength Concrete. *Journal of Structural Engineering* **125:3**,281-289.